

Theis, Winfried; Webber, Oliver; Weihs, Claus

**Working Paper**

## Statistics, dynamics and quality: Improving BTA-deep-hole drilling

Technical Report, No. 2004,06

**Provided in Cooperation with:**

Collaborative Research Center 'Reduction of Complexity in Multivariate Data Structures' (SFB 475), University of Dortmund

Suggested Citation: Theis, Winfried; Webber, Oliver; Weihs, Claus (2004) : Statistics, dynamics and quality: Improving BTA-deep-hole drilling, Technical Report, No. 2004,06, Universität Dortmund, Sonderforschungsbereich 475 - Komplexitätsreduktion in Multivariaten Datenstrukturen, Dortmund

This Version is available at:

<http://hdl.handle.net/10419/49350>

**Standard-Nutzungsbedingungen:**

Die Dokumente auf EconStor dürfen zu eigenen wissenschaftlichen Zwecken und zum Privatgebrauch gespeichert und kopiert werden.

Sie dürfen die Dokumente nicht für öffentliche oder kommerzielle Zwecke vervielfältigen, öffentlich ausstellen, öffentlich zugänglich machen, vertreiben oder anderweitig nutzen.

Sofern die Verfasser die Dokumente unter Open-Content-Lizenzen (insbesondere CC-Lizenzen) zur Verfügung gestellt haben sollten, gelten abweichend von diesen Nutzungsbedingungen die in der dort genannten Lizenz gewährten Nutzungsrechte.

**Terms of use:**

*Documents in EconStor may be saved and copied for your personal and scholarly purposes.*

*You are not to copy documents for public or commercial purposes, to exhibit the documents publicly, to make them publicly available on the internet, or to distribute or otherwise use the documents in public.*

*If the documents have been made available under an Open Content Licence (especially Creative Commons Licences), you may exercise further usage rights as specified in the indicated licence.*

# Statistics, Dynamics and Quality — Improving BTA-deep-hole drilling

Winfried Theis, Oliver Webber and Claus Weihs

January 13, 2004

In this paper we present how statistical experimental design, time series analysis and non-linear dynamic models have been applied to gain a deeper insight into BTA-deep-hole drilling process. BTA deep-hole drilling is used to produce long holes of a length to diameter ratio larger than 5. This process normally produces holes of high quality with regard to straightness, smoothness of the boring walls and roundness. However, two dynamic disturbances, chatter and spiralling, are sometimes observed in this process. While chatter mainly results in increased wear of the cutting edges of the tool but may also damage the boring walls, spiralling damages the workpiece severely.

In our study we applied experimental design to gain insight into the connection between process parameters and quality measures like roughness and roundness, while at the same time creating a database for dynamic modelling of the process. This turned out to be a very helpful approach because we observed all kinds of different dynamic disturbances. In this paper we will focus on chatter which turned out to be dominated by a few (eigen-) frequencies. Two models were proposed to describe the variation of the amplitudes of these frequencies, on the one hand a stochastic differential equation and on the other hand a descriptive model based on piecewise periodograms. In the latter model the knowledge of the underlying experimental design was used to distinguish between effects of the assembly of the machine, like damping by the starting bush on the tool, and effects of the dynamics and stochastic influences. Because this model is completely data-driven it can be used as a starting point for the development of a suitable dynamic model of a process.

## 1 Introduction

The work presented in this paper has been carried out as part of a project aimed at modelling the BTA deep hole drilling process, with special emphasis on dynamic aspects.

The longterm goal is online-prediction of dynamic disturbances which in future may be used as a basis for intelligent control of the process.

Deep hole drilling methods are used for producing holes with a high length-to-diameter ratio, good surface finish and straightness. For drilling holes with a diameter of 20 mm and above, the BTA (Boring and Trepanning Association) deep hole machining principle is usually employed (VDI, 1974). The working principle is shown in Figure 1.

In contrast to conventional twist drills, deep hole tools have an asymmetric cutting edge arrangement, resulting in a nonzero radial component of the cutting force. Through the radial component of the cutting force and the guiding pads indicated in Figure 1, a self guiding effect of the tool within the bore hole is achieved. This leads to a very low deviation of the bore hole axis from the ideal straight line. Another improvement over conventional drilling tools is the forced removal of the generated chips by the cutting fluid supplied at a high flow rate. These two aspects are prerequisites for deep hole drilling.

The machining of bore holes with a high length-to-diameter ratio implies the use of slender tool-boring bar assemblies featuring low static and dynamic stiffness properties. This in turn leads to the process being susceptible to dynamic disturbances such as chatter vibration, resulting in increased tool wear and in extreme cases leads to marks in the bore wall, and spiralling, which leads to a multi-lobe-shaped deviation of the cross section of the hole from absolute roundness (Fig. 2). The defects of form and surface quality constitute a significant impairment of the workpiece. As the deep drilling process is often used during the last production phases of expensive workpieces, process reliability is of prime importance. To achieve an optimal process design with the aim of reducing the risk of workpiece damage, a detailed analysis of the process dynamics is necessary.

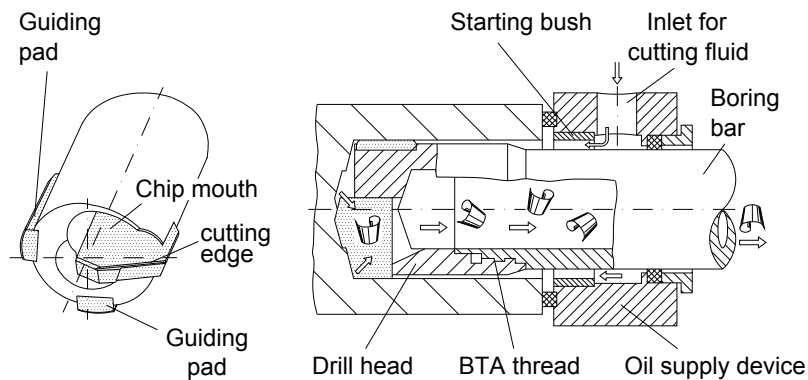


Figure 1: BTA deep hole drilling, working principle (VDI, 1974).

The investigation so far mainly focused on chatter vibration. The experiments were carried out on a system without additional damping in order to be able to observe the

unrestrained system dynamics. Current work in progress includes experiments with the addition of a Lanchester damper and the investigation of spiralling.

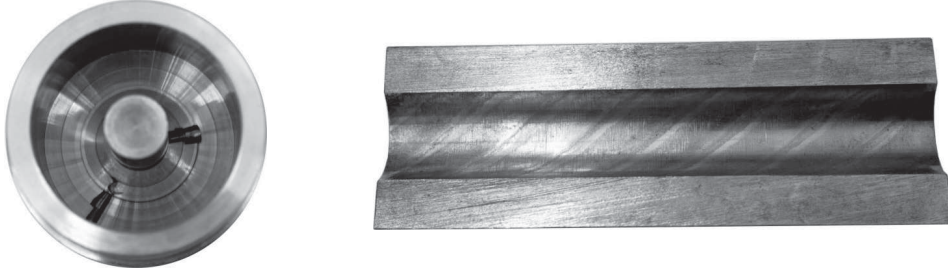


Figure 2: Radial chatter marks and effects of spiralling on the bore hole wall.

The paper is organised as follows: First we give a more detailed description of the experimental setup and the experimental design. Then in Section 4 we describe first explorative results on the on-line measurements of the drilling torque. Section 5 describes the dynamic phenomenological model and the descriptive model we derived from the observations. After this we discuss the results found by regressions of the influences on the parameters in the descriptive model and show connections to the structure of the machine. Finally the experiences with this approach are summarised in a conclusion.

## 2 Experimental Setup

The experiments were carried out on a CNC BTA deep hole drilling machine Type Giana GGB 560 with a bed length of 10.4 m, maximum spindle speed of 1600 1/min, maximum feed rate of 5700 mm/min and a maximum spindle power of 130 kW. The workpiece material used was C 60. A commercially available multi-edge BTA solid boring tool has been employed. It is equipped with three guide pads and two cutting inserts and has a nominal external diameter of 60 mm. Due to signal lines having to be lead away from the boring bar (see below), the experiments were carried out with stationary tool and rotating workpiece.

For the purpose of modelling the dynamics of BTA deep hole drilling, time series of quantities characterizing the process have to be recorded. Chatter and spiralling can be detected in the variation of the cutting and friction forces acting upon the cutting parts and guide pads respectively. These process forces were measured in terms of feed force and drilling torque transmitted via the boring bar. For this purpose, the strain gauges HBM Type XY11 6/120 and HBM Type XY21 6/120 were applied to the clamped end of the bar.

Airborne and structure-borne sound from several locations on the machine structure were also recorded. A diagram showing the experimental setup is given in Figure 4. The analysis presented in this paper focuses on the the torque data, which has proven to be the most expressive.

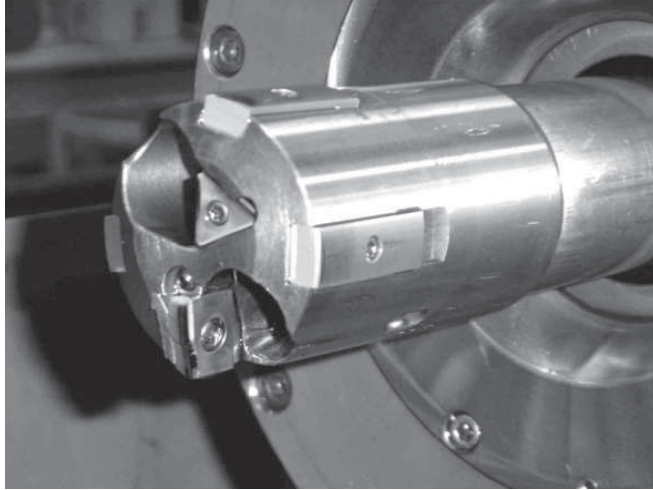


Figure 3: The BTA-tool used for the investigations.

In order to aid the interpretation of the process dynamics, the torsional modes of the tool-boring bar assembly were identified. For this purpose, the mounted tool was rotationally excited by impact offset from the center axis. The torsional response of the system was determined by evaluating the difference of the output of two acceleration sensors measuring in tangential direction and mounted diametrically opposed to each other on the boring head. By averaging the power spectra of five response measurements a spectrum was calculated from which the frequencies belonging to the first six torsional modes were identified.

### 3 Experimental Design

The first goal of the experimental design was to model quality measures of the process, which are the roughness of the bore hole wall and the roundness of the wall. We chose a quadratic function in three influencing factors, namely the cutting speed  $v_c$ , the feed  $f$  and the oil flow rate  $\dot{V}$ . These factors had turned out to be important influences on roughness, roundness and tool-wear in work of Astakhov et al. (1997a,b).

To be able to estimate this model a central-composite design was chosen with parameter  $\alpha = \sqrt{2}$  and seven repetitions in the center (Box and Draper, 1987). The design is depicted in a projection into the possible values of cutting speed and feed in Figure 5. As can be seen from this figure, one of the advantages of this design is the fact that only one influencing factor is set to an extreme value in the outlying experiments.

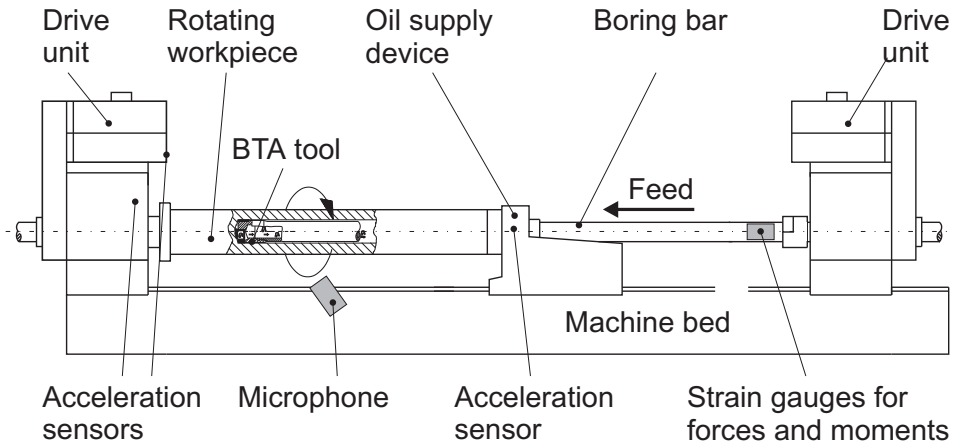


Figure 4: Experimental Setup.

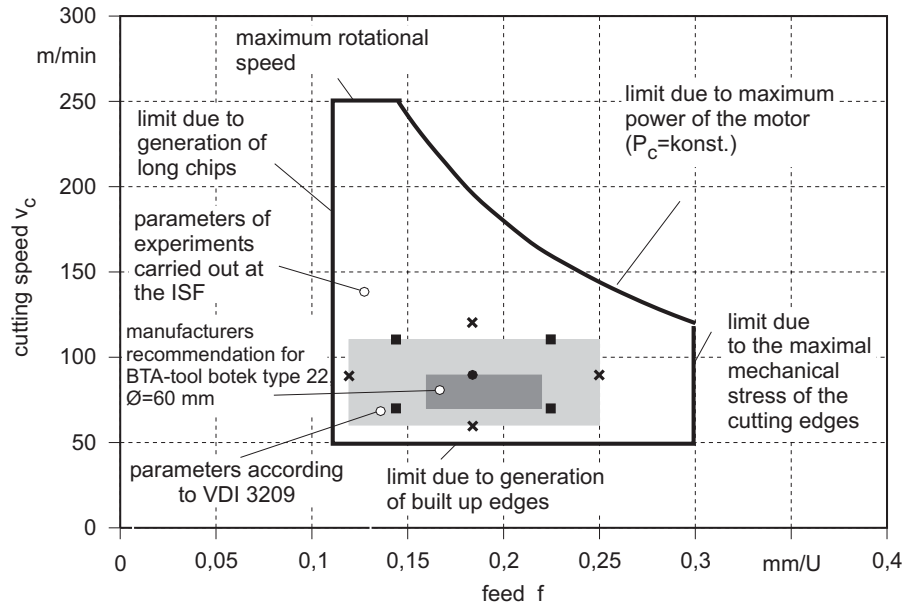


Figure 5: The experimental design in the space of the possible values of  $v_c$  and  $f$ .

The following values were chosen as extreme values for the three influencing factors:

	$f$	$v_c$	$\dot{V}$
min.	0.12	60	200
max.	0.25	120	400

Table 1: Extreme values of the influencing parameters.

Finally to allow for a possible influence of the wear of the cutting edge, the experiments were arranged in blocks by the number of experiments carried out on each cutting insert. Therefore, seven inserts were used and the observations were blocked into three groups.

We do not present the results on the quality measures in this paper, they can be found in Weinert et al. (2002).

## 4 Results from On-line Measurements

Phases with different process dynamics were observed during the experiments. These correspond with sections of the workpiece which also showed different characteristics.

Since the on-line measurements were to be explored with respect to the possibility to explain, understand and forecast chatter, the first approach was to look at spectrograms of the drilling torque. It transpired that different marks on the bore hole wall correspond to regimes of different frequencies. Figure 6 (b) shows an experiment at the center point of the experimental design, where two dynamic regimes are recognizable: in the first part of the process a frequency near 1200Hz is prominent and then slowly a second frequency near 700Hz becomes visible and finally dominates the process to the end. In Figure 6 (a) only chatter near 700Hz establishes after 300mm.

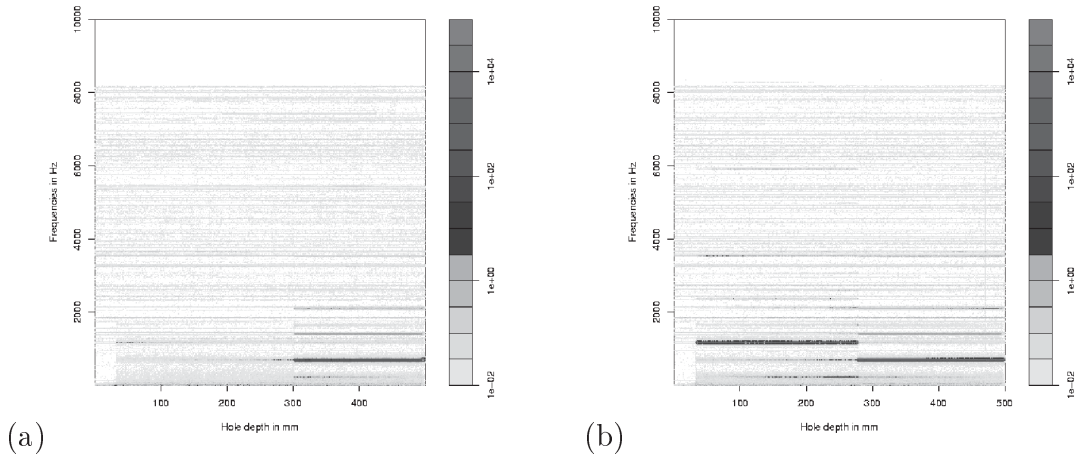


Figure 6: Spectrograms of two experiments at the center point of the design; (a) Chatter at the end (b) Chatter right after guide pads leave starting bush

These pictures clearly show that the process is dominated by single frequencies when chatter vibrations are present. This led to the ideas for the two models we consider here.

Which frequencies are relevant was determined by standardising the data (i.e. subtracting the mean and dividing by the standard deviation), then calculating the periodogram on sequences of length 4096 observations, and testing the periodogram ordinates against the standard exponential 95%-quantile. Frequencies with more than ten

rejections in six experiments were defined relevant. In Theis (2002) a more sophisticated method was proposed but to ensure comparability to earlier results we used the above method.

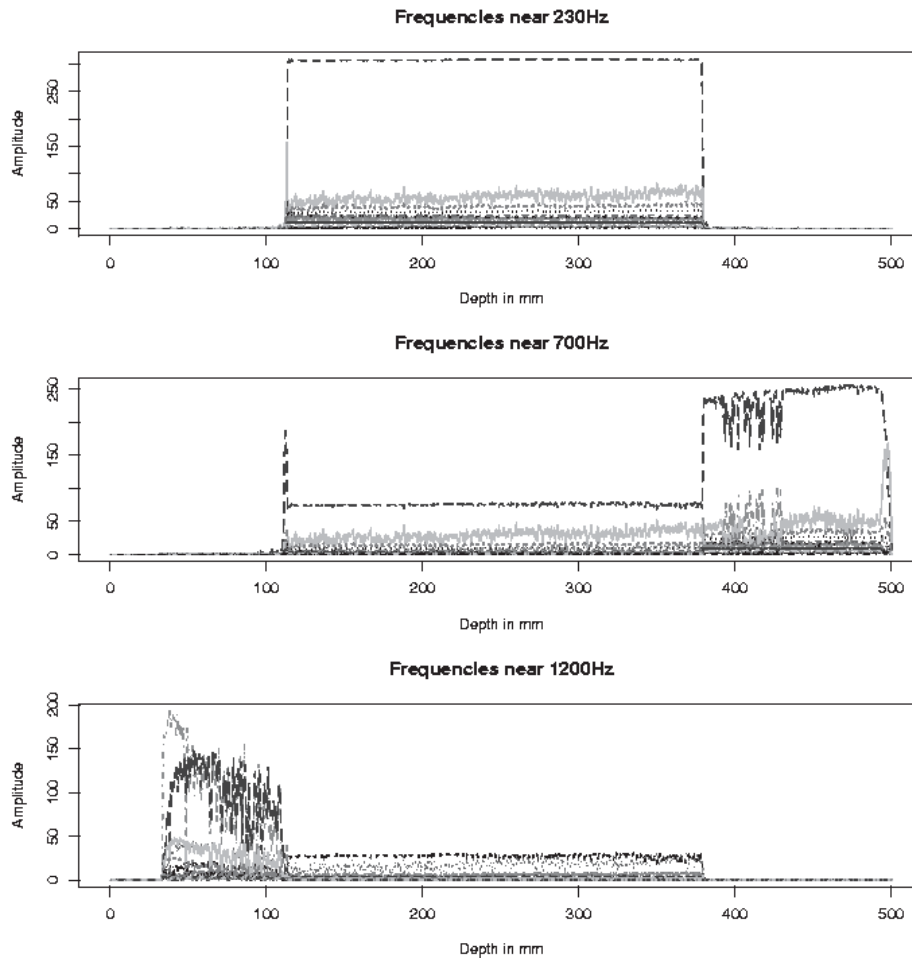


Figure 7: Variation of the amplitudes for frequencies top: 190-273Hz, middle: 659-747 Hz, and bottom: 1143-1406 Hz

When looking at the plots over time for various experiments it turns out that all these developments over time exhibit a common behaviour:

While the guiding pads are still in the starting bush none of the frequencies are significant, because the amplitudes are constraint by the fact that the tool is highly damped by contact with the starting bush. When the guiding pads leave the starting bush there is always an increase in all relevant amplitudes caused by freeing the tool. In most frequencies this increase takes the course of directly being damped again, forming a peak in the beginning and then declining again. Under some experimental conditions certain frequencies increase very quickly which leads to chatter right after the start of



the process. This chatter continues for some time until another frequency increases over a threshold and takes over the domination of the process. The first chatter always establishes near 1200 Hz while the second chatter can be near to 230Hz or 700 Hz. Stable chatter over the complete process is only observed when all relevant frequencies emerge directly after the guiding pads have left the starting bush.

For a better impression of this behaviour consider Figure 7, where the described behaviour can be seen.

## 5 Two Models

### Phenomenological model

As a general model for the description of the chatter in one frequency the following differential equation was proposed by Weinert et al. (2002):

$$\frac{d^2 M(t)}{dt^2} + h(t)(b^2 - M(t)^2) \frac{dM(t)}{dt} + \omega^2 M(t) = W(t) \quad (\text{i})$$

In a first step, this equation is considerably simplified, when  $M(t)$  is taken as harmonic process, eg.  $M(t) = g(t)\cos(2\pi f + \phi)$ . It follows for the amplitude that

$$2 \frac{dg(t)}{dt} + h(t)g(t)(b^2 - \frac{g(t)^2}{2}) = \frac{W(t)}{\omega}. \quad (\text{ii})$$

This is the amplitude-equation for the differential equation in (i), if there is only one frequency in the process. This model proved to generate behaviour very similar to the observed time series of the drilling torque, where only one chatter state was observed.

### Descriptive model

A descriptive model for the development of the amplitudes has to be flexible enough to be able to approximate all observed behaviour patterns of the process. Furthermore, it must be easy to parameterize with a small number of parameters to keep the complexity small and avoid over-fitting. The observed behaviour has as the most significant feature two different forms: On the one hand the fast jump to a maximal value and then decline back to the start level in a similarly steep descent, on the other hand a smaller peak and then a slow descent to the start level. When searching for a functional form which allows for both behaviours and is quite smooth, the idea came up to use a three parametric logistic function, which allows for steep rise, and multiply it with a logistic function on  $-x$  to allow for the descending behaviour.

So the basic functional form for the model is the following:

$$g(t; a, \mathbf{m}, \mathbf{d}) = \frac{a}{1 + \exp\left(\frac{-t+m_1}{d_1}\right) + \exp\left(\frac{t-m_2}{d_2}\right) + \exp\left(-\frac{(d_2-d_1)t+d_1 m_2-d_2 m_1}{d_1 d_2}\right)} \quad (\text{iii})$$

The following Figure 8 shows two parameter settings for this function, which exhibit the requested behaviour.

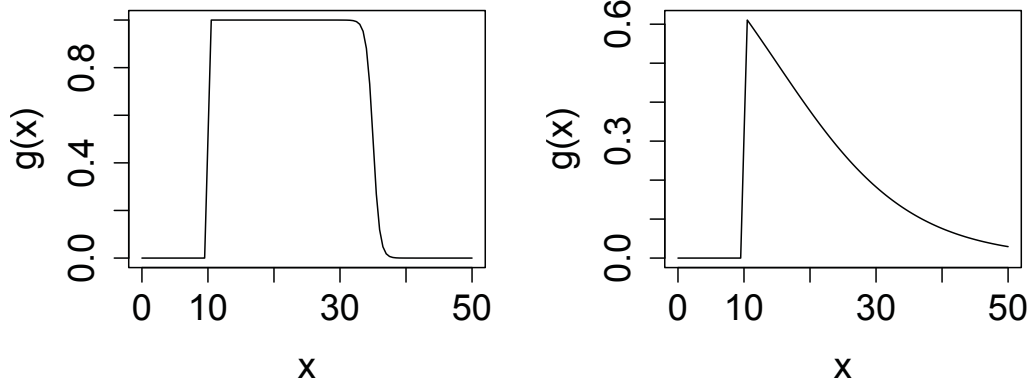


Figure 8:  $g(x; a, \mathbf{m}, \mathbf{d})$  for  $m_1 = 10$ ,  $m_2 = 40$ , and  $d_1 = 2 = d_2$  on the left-hand side, and  $m_{1,2} = 10$  and  $d_1 = 2$  and  $d_2 = 1000$  on the right-hand side.

Since in some experiments several changes in the chatter frequencies were observed, this should be incorporated by summing over several functions of this form. So the complete model to be fitted to the amplitudes over time reads:

$$G_k(t; \mathbf{a}, \mathbf{m}, \mathbf{d}) = \begin{cases} \mu_{A,k} & , \text{ for } t < 30\text{mm} \\ \mu_k + \sum_{j=1}^J \frac{a_{j,k}}{\left(1 + \exp\left(\frac{-t+m_{1,j,k}}{d_{1,j,k}}\right)\right) \left(1 + \exp\left(\frac{t-m_{2,j,k}}{d_{2,j,k}}\right)\right)} & , \text{ else.} \end{cases}$$

### Connection of the models

The descriptive model should be connected to the phenomenological model, so that it is possible to infer from connections of the machine parameters to the parameters of the descriptive model on similar connections of the parameters in the phenomenological model.

So assume that the logistic function is the right form for  $g(t)$ . Then it has to be shown that there is a function  $h(t)$  so that equation (ii) has a solution. To show this, the white noise is replaced by 0 to make the calculations more straightforward.

Set

$$g(t) := \frac{a}{1 + \exp\left(-\frac{t-t_0}{d}\right)},$$

it follows

$$\frac{dg(t)}{dt} = \left(-\frac{\exp\left(-\frac{t-t_0}{d}\right)}{d}\right) \frac{a}{\left(1 + \exp\left(-\frac{t-t_0}{d}\right)\right)^2}.$$

Inserting these formulas into (ii) we get

$$-2 \frac{\exp\left(-\frac{t-t_0}{d}\right) a}{d \left(1 + \exp\left(-\frac{t-t_0}{d}\right)\right)^2} + h(t) \left( \frac{ab^2}{1 + \exp\left(-\frac{t-t_0}{d}\right)} - \frac{a^3}{2 \left(1 + \exp\left(-\frac{t-t_0}{d}\right)\right)^3} \right) = 0$$

Adding the first term on both sides:

$$h(t) \left( \frac{2ab^2 \left(1 + \exp\left(-\frac{t-t_0}{d}\right)\right)^2 - a^3}{2 \left(1 + \exp\left(-\frac{t-t_0}{d}\right)\right)^3} \right) = 2 \frac{\exp\left(-\frac{t-t_0}{d}\right) a}{d \left(1 + \exp\left(-\frac{t-t_0}{d}\right)\right)^2}.$$

Because the term in brackets on the left hand side is never 0, it is possible to divide by it. It follows

$$h(t) = 2 \frac{\exp\left(-\frac{t-t_0}{d}\right) \left(1 + \exp\left(-\frac{t-t_0}{d}\right)\right)}{d \left(b^2 \left(1 + \exp\left(-\frac{t-t_0}{d}\right)\right)^2 - \frac{a^2}{2}\right)}$$

This solution is well-defined for  $t \in \mathbb{R}$ . So  $(g, h)$  is a pair of functions, which solves equation (ii).

## 6 Results on Amplitudes

### Connections to machine parameters

One interesting question regarding the behaviour of the amplitudes at the relevant frequencies was whether there are features which are influenced by the machine parameters. The maximal value of the amplitudes was an obvious choice because it is bounded by the damping factor of the tool/workpiece assembly and the amount of energy introduced into the system by force, cutting speed and the flow rate of the oil.

So for each experiment and each relevant frequency the maximal value was determined. The maximal values for each frequency were regressed on the three machine parameters used in the experimental design. For each frequency the best fitting model was searched for by stepwise regression based on AIC starting with the quadratic model with all interactions up to the three factor interaction. In Tables 2, 3 and 4 the chosen parameters are reported and marked if they are significant by "X". Interesting about these models is that the three main important frequency bands are dominated each by a different group of machine parameters. For the low frequency chatter around 240Hz these parameters are the feed  $f$  and the flow rate of the oil  $\dot{V}$  which are significant in most of the models in which they are present (13 of 18, and 13 of 16, resp.). The feed  $f$  comes in also as quadratic term in some models. In this frequency band the cutting speed  $v_c$  is present by the interaction  $f : v_c$  and the quadratic term  $v_c^2$ . in a significant way (4 of 16).

Hz	$\mu$	$f^2$	$v_c^2$	$\dot{V}^2$	$f$	$v_c$	$\dot{V}$	$f : v_c$	$f : \dot{V}$	$v_c : \dot{V}$	$f : v_c : \dot{V}$	$R_{adj.}^2$	AIC
5	.	+	.	.	+	+	X	+	+	.	.	0.375	12.05
190	X	.	.	+	X	+	X	+	+	.	.	0.449	15.462
195	X	.	.	.	X	+	X	+	+	.	.	0.409	41.512
200	X	.	.	.	X	+	X	+	+	.	.	0.371	61.951
205	X	.	.	.	X	+	X	+	+	.	.	0.346	77.551
210	X	.	.	.	X	+	X	+	+	.	.	0.307	89.84
215	.	+	.	.	+	+	+	+	+	.	.	0.265	99.139
220	.	+	+	.	+	+	+	+	+	.	.	0.201	105.444
225	.	X	X	.	X	X	.	.	.	.	.	0.134	107.497
229	X	X	X	.	+	X	+	X	+	.	.	0.644	100.05
<b>234</b>	X	.	.	.	X	+	X	+	+	.	.	0.341	219.559
<b>239</b>	X	.	.	+	X	+	X	X	+	.	.	0.464	162.548
<b>244</b>	X	.	.	.	X	+	X	X	+	.	.	0.452	134.846
<b>249</b>	X	.	.	.	X	+	X	X	+	.	.	0.411	120.458
<b>254</b>	X	.	.	.	X	+	X	+	+	.	.	0.369	106.944
259	X	.	.	.	X	+	X	+	+	.	.	0.334	91.925
264	.	+	.	.	+	+	X	+	+	.	.	0.318	73.434
269	.	+	+	.	+	+	+	+	+	.	.	0.232	51.373
273	.	X	X	.	X	+	.	.	.	.	.	0.139	18.803

Table 2: Results of the stepwise regressions on the maximal amplitudes per relevant frequency in the lower frequency bands. “+” means chosen for the model, but not significant on a 10% level, “X” means significant influence.

For the chatter around 700Hz the most dominant parameters are the feed  $f$ , the cutting speed  $v_c$  and their interaction  $f : v_c$ . The most frequently significant quadratic term is the feed (5 of 6). The flow rate of the oil is only present in 8 of 16 models and only in two of them significant.

Hz	$\mu$	$f^2$	$v_c^2$	$\dot{V}^2$	$f$	$v_c$	$\dot{V}$	$f : v_c$	$f : \dot{V}$	$v_c : \dot{V}$	$f : v_c : \dot{V}$	$R_{adj.}^2$	AIC
469	.	.	.	.	+	+	+	+	.	.	.	0.133	53.028
474	.	.	+	+	X	+	+	X	.	.	.	0.482	15.014
659	X	X	+	.	+	X	+	X	+	.	.	0.334	-3.84
664	X	.	.	.	X	X	.	X	.	.	.	0.302	16.625
669	X	.	.	.	X	X	.	X	.	.	.	0.277	35.82
<b>674</b>	.	.	.	.	X	X	.	X	.	.	.	0.216	53.426
<b>679</b>	X	.	.	.	+	X	+	X	.	+	.	0.164	69.533
<b>684</b>	.	.	.	.	.	.	.	.	.	.	.	#	#
<b>688</b>	.	.	.	.	.	.	.	.	.	.	.	#	#
<b>693</b>	X	+	.	.	X	X	X	X	X	X	X	0.226	90.304
<b>698</b>	X	X	.	.	X	X	X	X	X	X	X	0.717	121.477
<b>703</b>	.	.	.	.	+	X	.	X	.	.	.	0.239	191.567
<b>708</b>	.	X	X	.	X	X	.	.	.	.	.	0.473	145.699
<b>713</b>	.	X	X	.	+	X	.	X	.	.	.	0.436	108.577
<b>718</b>	.	.	.	.	X	X	.	X	.	.	.	0.306	94.635
<b>723</b>	.	.	.	.	+	X	.	X	.	.	.	0.251	82.319
<b>728</b>	X	.	.	.	+	X	+	X	.	+	.	0.203	70.947
<b>732</b>	.	.	.	.	.	.	.	.	.	.	.	#	#
<b>737</b>	.	.	.	.	.	.	.	.	.	.	.	#	#
<b>742</b>	.	.	.	.	.	.	.	.	.	.	.	#	#
747	.	X	+	.	+	X	+	+	X	+	+	0.271	-14.619

Table 3: Results of the stepwise regressions on the maximal amplitudes per relevant frequency in the middle frequency bands. “+” means chosen for the model, but not significant on a 10% level, “X” means significant influence. Frequencies with # as result for  $R_{adj.}^2$  and AIC gave no sensible model at all.

In the models for the frequency band around 1200Hz the clearly dominating machine parameter is the cutting speed  $v_c$ , which is present in all models and in some additionally as quadratic term. The flow rate of the oil  $\dot{V}$  is the second interesting parameter in this frequency band with 7 selections in the 16 models.

Finally the frequencies near 1650Hz display a clear common behaviour with  $\dot{V}^2$ , all main effects and interaction  $f : v_c$  present in all models. All frequency bands not mentioned do not display a clear pattern.

Hz	$\mu$	$f^2$	$v_c^2$	$\dot{V}^2$	$f$	$v_c$	$\dot{V}$	$f : v_c$	$f : \dot{V}$	$v_c : \dot{V}$	$f : v_c : \dot{V}$	$R_{adj.}^2$	AIC
942	.	.	X	+	X	+	+	X	.	.	.	0.563	7.645
1143	X	.	.	.	.	X	.	.	.	.	.	0.403	17.272
<b>1147</b>	X	.	.	.	.	X	.	.	.	.	.	0.348	30.975
<b>1152</b>	.	.	.	.	.	X	.	.	.	.	.	0.246	43.836
<b>1157</b>	.	.	.	.	.	X	.	.	.	.	.	0.158	53.257
<b>1162</b>	.	.	.	.	.	.	.	.	.	.	.	#	#
<b>1167</b>	.	.	.	.	.	.	.	.	.	.	.	#	#
<b>1172</b>	.	+	.	.	+	+	.	+	.	.	.	0.258	102.813
<b>1177</b>	.	.	X	+	+	X	+	.	.	.	.	0.448	120.159
<b>1182</b>	.	.	+	+	.	X	+	.	.	.	.	0.304	194.61
<b>1187</b>	.	.	.	+	.	X	+	.	.	.	.	0.342	178.79
<b>1191</b>	X	.	.	.	.	X	.	.	.	.	.	0.34	126.508
<b>1196</b>	X	.	.	.	.	X	.	.	.	.	.	0.336	99.296
<b>1201</b>	X	.	.	.	.	X	.	.	.	.	.	0.269	79.079
<b>1206</b>	.	.	.	.	.	X	.	.	.	.	.	0.165	60.754
1211	X	.	+	.	.	X	.	.	.	.	.	0.184	37.581
1216	.	.	X	X	+	+	X	+	.	.	.	0.5	13.634
1221	.	.	+	X	+	+	X	X	.	.	.	0.51	11.068
1226	.	.	.	X	.	X	X	.	.	.	.	0.366	12.579
1406	.	.	.	.	.	+	X	.	.	+	.	0.131	24.558
1411	X	.	X	.	.	X	.	.	.	.	.	0.368	-5.703
1636	.	.	.	.	.	.	.	.	.	.	.	#	#
1641	.	.	.	.	.	.	.	.	.	.	.	#	#
1646	.	.	+	+	+	+	+	X	.	.	.	0.399	92.528
1650	X	.	.	X	X	X	X	X	.	.	.	0.637	54.582
1655	X	.	.	X	X	X	X	X	.	.	.	0.635	7.128
1660	X	.	.	X	X	X	X	X	+	.	.	0.662	-19.362
1665	X	.	.	+	X	X	X	X	+	.	.	0.628	-35.379
<b>2109</b>	.	.	.	.	+	X	X	.	.	X	.	0.109	35.858
<b>2114</b>	.	.	X	.	+	+	.	+	.	.	.	0.447	37.544
<b>2119</b>	X	.	.	+	X	X	+	X	.	.	.	0.534	41.262
2124	.	.	+	.	X	+	+	X	.	+	.	0.417	-19.344

Table 4: Results of the stepwise regressions on the maximal amplitudes per relevant frequency in the higher frequency bands. “+” means chosen for the model, but not significant on a 10% level, “X” means significant influence. Frequencies with # as result for  $R_{adj.}^2$  and AIC gave no sensible model at all.

These result have to be handled carefully because of the often low  $R_{adj.}^2$ . But at least they give hints, which parameters are more promising when trying to avoid a certain type of chatter.

After fitting the descriptive model to the amplitudes we regressed the parameters

$a, d_1, d_2$  of the basic functions with maximal  $a$  with a positive distance  $m_2 - m_1$  on the machine parameters. The parameter  $a$  behaves quite similar to the maximal values, for the other parameters no clear pattern could be established.

### Connections to the machine assembly

The parameters  $m_1$  and  $m_2$  describe the positions where the model finds a jump upwards or a descent, respectively. In the experiments at the center point we found very different behaviour patterns when chatter started. It was obvious that this is not directly connected to the machine parameters. So these parameters are evaluated more with the focus on more likely positions of changes in the dynamic state.

First the largest jumps – regardless if upwards or downwards – on all amplitudes over all experiments are counted on sections of  $5mm$  length and displayed in Figure 9.

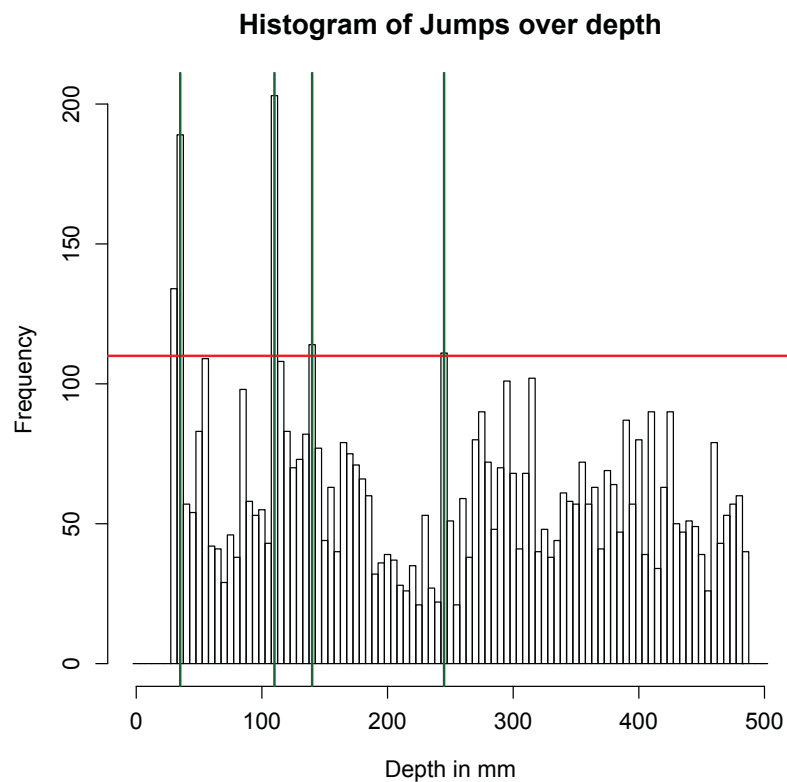


Figure 9: Number of frequencies with a jump in the amplitude within segments of  $5mm$ .

The vertical lines at depths  $35mm, 110mm, 140mm$  and  $250mm$  indicate the most prominent jumps apart from those at the end of the process. It could be argued that there are other bars which are only slightly below the horizontal line at 250 counts, like  $50/55mm, 85mm, 295mm, 325$  and  $385mm$ . The cut-off point of 250 counts is chosen to have only a few vertical lines to keep the structure of the plot visible.

It is interesting that the highest bar in the plot is at  $110mm$  and not at  $30/35mm$

depth. This position has also a meaning in the machine assembly. It is approximately the position where the tool enters the bore hole completely. This might lead to changes in the dynamic process because the boring bar is slightly thinner than the tool and therefore the pressures in the hole may change.

Comparing this to the results from the fits, we get the following histograms (Fig. 10 and 11) with some additional information on jumps up or down.

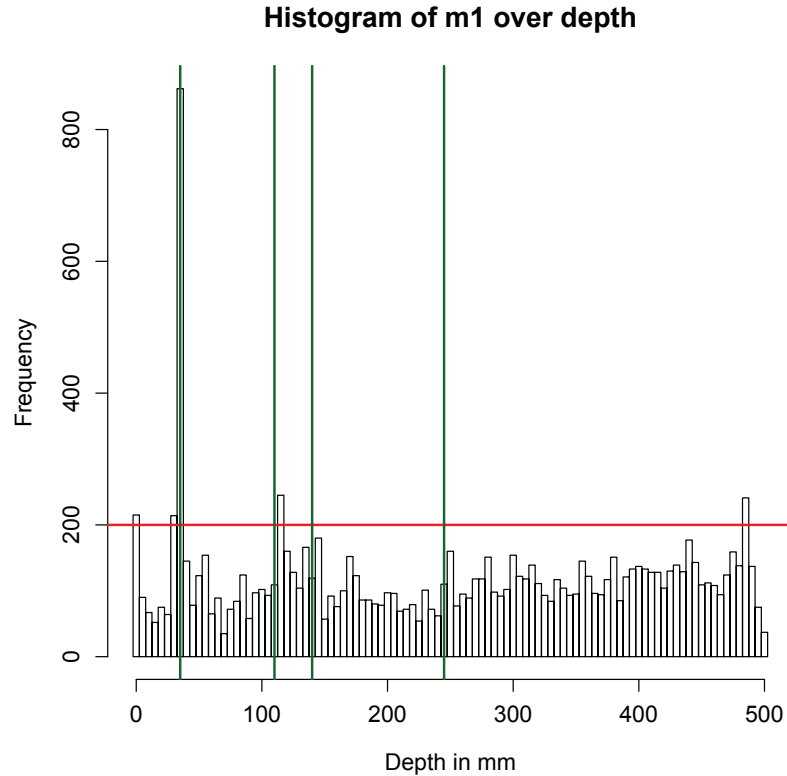


Figure 10: Number of fits of basic functions with a realisation of  $m_1$  within segments of  $5mm$ .

Compared to Figure 9 the depth of  $35mm$  has become in Figure 10 as important as expected. The depth  $110mm$  is still one of the highest bars, while  $140mm$  and  $250mm$  do not stand out any more. The same is true for all other depths named before. So upward jumps only happen more often at  $0mm$ ,  $35mm$ ,  $110mm$  and interestingly at  $485mm$  depth.



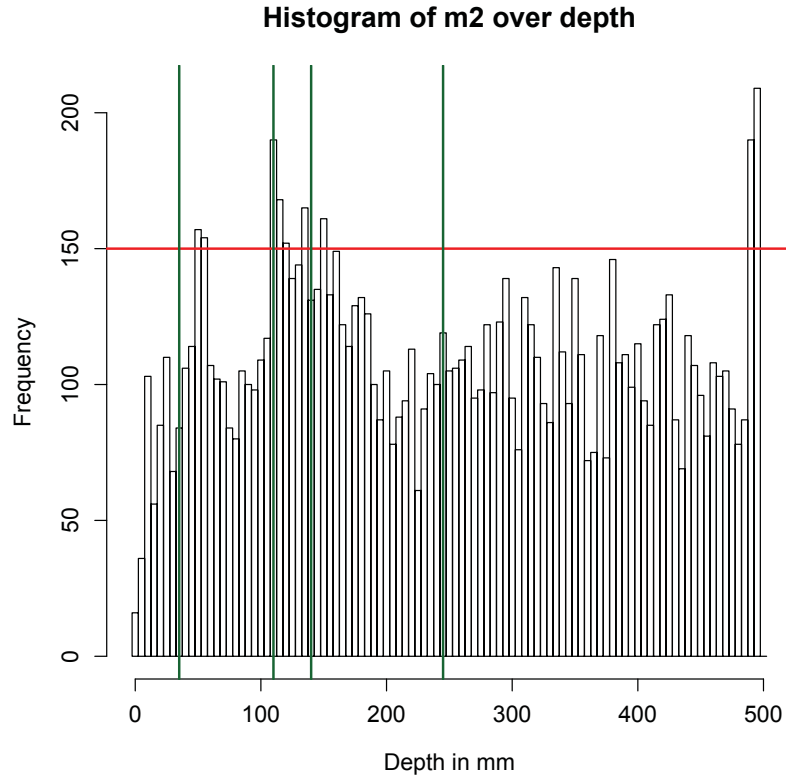


Figure 11: Number of fits of basic functions with a realisation of  $m_2$  within segments of  $5mm$ .

In Figure 11 it is obvious that the downward jumps are a bit more fuzzy than the upward jumps, because there are two types: On the one hand the slow descent from a peak and on the other hand the steep fall from a plateau. Here a possible explanation for the order of the number of counts in Figure 9 can be found: Depth  $35mm$  is only important for the rise, but depth  $110mm$  is important for rise and descent. In Histogram 11 all other peaks from Figure 9 not present in Figure 10 are present.

From this investigation it is obvious that the dynamic behaviour not only changes right after the guiding pads leave the starting bush but also at  $110mm$  which may be connected with the tool completely entering the workpiece at approximately this drilling depth.

### Predicting early Chatter by Fitted Values

One of the challenging problems encountered when modelling the BTA deep-hole drilling process is the chatter vibrations starting directly after the guiding pads leave the starting bush. So we tried to use the fitted values of the varying amplitudes to predict whether it is likely that there will be such chatter vibration or not.

This problem was analysed as a classification problem. The 22 experiments (one experiment produced usable data but was repeated because of a damaged cutting edge)

were classified into two groups – chatter vibration right after the guiding pads leave the starting bush (16 observations) and no such chatter (6 observations). On the frequencies highly significant in most experiments (marked boldface in Tabulars 2 to 4) the median of the fitted values between 25mm and 35mm depth was calculated. The high frequencies appeared more important because the strong damping by the starting bush only allows small movements of the tool.

The small number of observations especially in the group with no chatter restricted the choice of the classification method. We chose the well-known linear discriminant analysis (LDA) (cf. e.g. Venables and Ripley (2002) pp. 332-339) because it is one of the most stable methods and hard to beat with respect to prediction ability even in difficult situations (cf. Pouwels et al. (2002)). Because the number of classifier variables is still too high with 37 variables a stepwise variable selection procedure based on a 4-fold crossvalidation was performed.

The described procedure led to the following set of frequencies to classify the experiments into early chatter or none: 234Hz, 249Hz, 2109Hz, 2114Hz and 2119Hz. With this set of classifier variables a leave-one-out error rate of 13.6% was reached. A closer inspection of the posterior probability for the classes showed that one of the three wrong classifications was based on 50.4% for the wrong class. Therefore, we decided to check whether the discrimination could be improved by adding the machine parameters to the set of discriminators and using again the variable selection procedure. This led to the inclusion of the cutting speed into the variable set which led to the correct classification of the above mentioned observation. With this final set of variables the leave-one-out error rate was reduced to 9.1% and the two wrongly assigned observations were assigned to the class of no chatter.

## 7 Conclusions

The usage of an experimental design made it possible to investigate the effect of the machine parameters on the parameters of the descriptive model. The repetitions in the center point of the central-composite design made clear that the depths where the dynamic state of the process changes are not influenced by the machine parameters. Moreover, it makes it possible to see that some of the points where the dynamic state changes are connected to depths, which certain structures of the tool–boring bar assembly can be assigned to.

Generally the central-composite design is not the best possible design for such an investigation of the dynamics of a process. For similar investigations we would propose to use repeated space filling designs (like eg. Coffee-House-Designs Müller (2001)) to get more insight into the dynamics at each experimental setting and even a broader selection of these settings.

The results from these investigations can be used in our project to derive control actions for different kinds of chatter. Especially the clear patterns of influences on the maximal amplitudes can be used to formulate a specific reactions on appropriate signals from the observation of the amplitudes.

The second very important result of these investigations is the very good discrimination between chatter right after the guiding pads leave the starting bush against no such chatter by the use of the frequencies 234Hz, 249Hz, 2109Hz, 2114Hz and 2119Hz as discriminating variables. This makes it possible to use these signals to account also for this special kind of chatter.

## Acknowledgements

This work has been supported by the Collaborative Research Centre “Reduction of Complexity in Multivariate Data Structures” (SFB 475) of the German Research Foundation (DFG).

## References

- V.P. Astakhov, M.O.M. Osman, and M. Al-Ata. Statistical design of experiments in metal cutting – part one: Methodology. *Journal of Testing and Evaluation*, 25(3): 322–327, 1997a.
- V.P. Astakhov, M.O.M. Osman, and M. Al-Ata. Statistical design of experiments in metal cutting – part two: Applications. *Journal of Testing and Evaluation*, 25(3): 327–335, 1997b.
- G.E.P. Box and N.R. Draper. *Empirical Model-Building and Response Surfaces*. Wiley & Sons, New York, 1987.
- W. G. Müller. Coffee-house designs. In A. Atkinson et al., editor, *Optimum Design 2000*, pages 241–248. Kluwer Academic Publishers, 2001.
- Britta Pouwels, Winfried Theis, and Christian Röver. Implementing a new method for discriminant analysis when group covariance matrices are nearly singular. In Martin Schader, Wolfgang Gaul, and Maurizio Vichi, editors, *Between Data Science And Applied Data Analysis*, pages 92–99. Gesellschaft für Klassifikation, Springer, 2002.
- Winfried Theis. Design of experiments for static influences on harmonic processes. Technical Report 60, Collaborative Research Center 475, Universität Dortmund, 2002.
- VDI. Tiefbohrverfahren. *VDI Düsseldorf*, 1974.
- W.N. Venables and B.D. Ripley. *Modern Applied Statistics with S*. Springer, 4<sup>th</sup> edition, 2002.
- K. Weinert, O. Webber, M. Hüsken, J. Mehnen, and W. Theis. Analysis and prediction of dynamic disturbances of the bta deep hole drilling process. In R. Teti, editor, *Proceedings of the 3<sup>rd</sup> CIRP International Seminar on Intelligent Computation in Manufacturing Engineering*, 2002.